Wiley
Journal of Probability and Statistics
Volume 2026, Article ID 4060053, 17 pages
https://doi.org/10.1155/jpas/4060053

WILEY

Research Article

The Modified Fréchet-Exponentiated Exponential Distribution: Novel Model for Reliability and Survival Analysis

Merga Abdissa Aga,[1] **Shibiru Jabessa Dugasa**,[2] **Habte Tadese**,[3,4] **and Ding-Geng Chen**[4,5]

[1]*Department of Statistics, Salale University, Fiche, Ethiopia*
[2]*Department of Statistics, Wollega University, Nekemte, Ethiopia*
[3]*Department of Statistics, Addis Ababa University, Addis Ababa, Ethiopia*
[4]*College of Health Solutions, Arizona State University, Phoenix, Arizona, USA*
[5]*Department of Statistics, University of Pretoria, Pretoria, South Africa*

Correspondence should be addressed to Merga Abdissa Aga; mergabdisa3@gmail.com

Received 29 October 2025; Revised 4 December 2025; Accepted 24 December 2025

Academic Editor: Ramón M. Rodríguez-Dagnino

This study introduces a novel statistical model called the modified Fréchet-exponentiated exponential (MFrEE) distribution. The existing exponentiated exponential (EE) distribution, while useful for lifetime and reliability data, has limited flexibility in capturing diverse hazard shapes and may not adequately model extreme events or tail behavior. To address these limitations, the MFrEE distribution applies a modified Fréchet generator to the EE baseline, enhancing the model's flexibility and robustness. Its survival and hazard functions, cumulative distribution function, and probability density function are derived, presented, and illustrated with plots for various parameter values. The study provides a comprehensive mathematical analysis of the distribution, deriving its moments, mean, variance, quantiles, and moment-generating function. Methodologically, the model is simulated using an accept–reject algorithm, and its parameters are estimated via maximum likelihood estimation (MLE). The performance of the estimators is assessed through Monte Carlo simulations using bias, mean squared error, and coverage probability (CP), with the CP results showing values close to the nominal 95% level across different parameter settings. Furthermore, the robustness and performance of the proposed method are evaluated using AIC, BIC, and AICc, demonstrating superior performance compared to baseline methods across three publicly available datasets. The study concludes by proposing this model as a significant contribution to probability theory and suggests two avenues for future research: applying the model to more real-world problems and using machine learning methods for parameter estimation to compare with the MLE approach used in this study.

Keywords: accept–rejection algorithm; maximum likelihood estimation; modified Fréchet-exponentiated exponential; simulation

1. Introduction

Modeling lifetime and survival data is a cornerstone of statistical analysis in numerous disciplines, such as reliability engineering, medical research, actuarial science, and risk management. Among the foundational models, the exponential distribution has played a pivotal role due to its mathematical simplicity and the memoryless property, making it a natural starting point for lifetime modeling [1]. However, the exponential model's assumption of a constant hazard rate severely limits its applicability in real-world scenarios, where hazard functions often vary with time.

To address this limitation, researchers introduced extensions such as the exponentiated exponential (EE) distribution (EED) [2], which incorporates an additional shape parameter to capture monotonic increasing or decreasing hazard rates. The EED demonstrated superior flexibility over the classical exponential model and has been applied

successfully across various fields [3, 4]. Nevertheless, the EE and many related models still fall short when confronting complex hazard shapes frequently observed in empirical data, including bathtub-shaped and unimodal hazard functions [5, 6].

This challenge has spurred the development of a rich variety of generalized and compound distributions aimed at expanding the modeling toolkit. Generator methods, which systematically transform a baseline distribution by introducing new parameters through functional compositions, have proven particularly fruitful [7, 8]. These methods enable the construction of flexible distribution families that better capture diverse empirical behaviors, including tail weight variation and skewness adjustment [9, 10].

In recent years, a wide range of fields—such as engineering, economics, biology, environmental sciences, insurance, finance, and lifetime analysis—have increasingly turned to these innovative families of distributions for modeling complex data. Notable developments include the exponentiated generalized-G family [11], the exponentiated transformed-transformer (T-X) family [12], and the T-X family [13], which have broadened the flexibility of classical models. Further research has explored contemporary extensions and applications across diverse datasets, as illustrated by Ahmad et al. [14, 15]; Al-Moisheer et al. [16]; Almarashi and Elgarhy [17]; Almarashi et al. [18]; Alyami, Babu et al. [19]; Alyami, Elbatal et al. [20]; Benchiha et al. [21]; and Elbatal, Elgarhy, and Kibria [22].

More recent innovations, such as the general weighted exponentiated family [23], the inverse unit exponential probability distribution [24], and the transmuted exponential power distribution [25], have further expanded modeling capabilities. Studies focusing on parameter estimation and advanced modeling strategies (Ahmadini et al. [26], Al-Babtain et al. [27], Alabdulhadi et al. [28], Alghamdi et al. [29], Alotaibi et al. [30], Alyami et al. [20], Eldessouky et al. [31], Gemeay et al. [32], Hassan et al. [33], Jamal et al. [34], Ragab et al. [35], Shrahili et al. [36]) have strengthened the practical applicability of these families. Collectively, these efforts underscore the rapid evolution of flexible lifetime models capable of accommodating complex hazard patterns, heavy tails, and skewed data.

Despite these advancements, several generalized exponential (GE)-type models remain limited in their ability to simultaneously model heavy tails and nonmonotonic hazard structures. For example, while the EE and GE distributions improve monotonic hazard flexibility, they cannot accommodate bathtub or unimodal hazards. The exponentiated Weibull and exponentiated power distributions provide more shape control but often fail to capture heavy-tailed behavior. Other transformer-based families—such as the exponentiated generalized-G, T-X exponential-based, and transmuted exponential power models—introduce additional parameters but still exhibit restricted tail behavior or lack closed-form expressions for key functions in some cases. Thus, there is a clear methodological gap for models that jointly allow: flexible tail behavior, multiple hazard shapes (increasing, decreasing, bathtub, unimodal), and mathematical properties enabling practical inference.

One recently proposed technique, the modified Fréchet generator, extends baseline distributions by integrating the Fréchet distribution's heavy-tail characteristics with a normalization adjustment to ensure a proper distribution [37, 38]. This generator enriches the shape flexibility, particularly enhancing tail behavior control and enabling the modeling of intricate hazard rate patterns such as increasing, decreasing, bathtub, and unimodal forms [39, 40]. Applications of this generator to classical families such as Weibull, Lindley, and gamma distributions have demonstrated marked improvements in fitting lifetime and reliability data [41].

Motivated by the need for more flexible and versatile lifetime models, this study introduces a novel distribution by applying the modified Fréchet generator to the EED, hereafter referred to as the modified Fréchet-exponentiated exponential (MFrEE) distribution. This newly proposed family combines the shape flexibility of the EE baseline with the tail- and hazard-shaping capabilities of the modified Fréchet generator, resulting in a model that can capture a wide variety of hazard rate behaviors—including nonmonotonic and bathtub-shaped hazards—frequently observed in reliability and survival studies.

In contrast to other GE-type models, the MFrEE distribution simultaneously provides extended tail flexibility via the Fréchet-based generator, enhanced hazard rate versatility beyond the EE baseline, and mathematical forms for density, hazard, and quantile functions, enabling straightforward inference and application.

The novelty of the MFrEE distribution lies in combining the EE baseline distribution with the modified Fréchet generator. While the EED already introduces flexibility in modeling lifetimes through its shape parameter, it has limitations in capturing complex tail behaviors and diverse hazard rate shapes that often arise in real-world data. To overcome these drawbacks, we applied the modified Fréchet generator, which introduces an additional parameter (γ) that significantly enhances the distribution's tail flexibility and allows for increasing, decreasing, bathtub-shaped, and upside-down bathtub-shaped hazard functions. This modification extends the modeling capability of the baseline distribution, ultimately boosting performance in fitting real datasets when compared to the state-of-the-art methods, such as the EED.

Moreover, the practical applicability of the MFrEE distribution is demonstrated through simulation studies and analyses of real-world datasets, showing that it outperforms existing models such as the Weibull, EE, and modified Weibull distributions. These results highlight the MFrEE model's ability to capture complex failure mechanisms more effectively and to improve inference in survival analysis, reliability engineering, and related fields.

This paper derives the MFrEE distribution's statistical properties—including the probability density, cumulative distribution, hazard rate, quantile function, and moments—and develops parameter estimation procedures using maximum likelihood methods while discussing asymptotic behavior and coverage probability (CP). Its performance is evaluated using simulated and real datasets,

demonstrating superior fit according to AIC, BIC, and AICc criteria.

The remainder of this paper is organized as follows: Section 2 presents the methodology and statistical properties of the MFrEE distribution. Section 3 provides simulation studies evaluating estimation performance. Section 3 demonstrates applications using real datasets, and Section 4 offers concluding remarks and directions for future research.

2. Methods

2.1. The MFrEE Distribution. Let X be a continuous random variable. The MFrEE distribution is constructed by applying the modified Fréchet generator to the baseline EED.

2.1.1. EED. The EED with parameters $\lambda > 0$ (scale) and $\alpha > 0$ (shape) has the cumulative distribution function (CDF) and probability density function (PDF) given by the following equations:

$$F_0(x;\lambda,\alpha) = \left(1 - e^{-\lambda x}\right)^{\alpha}, \quad x > 0, \tag{1}$$

$$f_0(x;\lambda,\alpha) = \alpha\lambda e^{-\lambda x}\left(1 - e^{-\lambda x}\right)^{\alpha-1}. \tag{2}$$

2.1.2. Modified Fréchet Generator. The modified Fréchet generator modifies any baseline CDF $F_0(x)$ by the transformation:

$$F(x) = \frac{e^{-(F_0(x))^{\gamma}} - 1}{e^{-1} - 1}, \quad \gamma > 0. \tag{3}$$

Ensuring $F(x)$ is a valid CDF on the support of X.

2.1.3. MFrEE Distribution. Applying the modified Fréchet generator to the EE baseline yields the MFrEE CDF:

$$F(x;\lambda,\alpha,\gamma) = \frac{e^{-\left(\left(1-e^{-\lambda x}\right)^{\alpha}\right)^{\gamma}} - 1}{e^{-1} - 1}, \quad x > 0, \tag{4}$$

and the PDF:

$$f(x;\lambda,\alpha,\gamma) = \frac{\gamma\alpha\lambda e^{-\lambda x}\left(1 - e^{-\lambda x}\right)^{\alpha-1}\left(\left(1 - e^{-\lambda x}\right)^{\alpha}\right)^{\gamma-1} e^{-\left(\left(1-e^{-\lambda x}\right)^{\alpha}\right)^{\gamma}}}{1 - e^{-1}}, \tag{5}$$

which is simplified as follows:

$$f(x;\lambda,\alpha,\gamma) = \frac{\gamma\alpha\lambda e^{-\lambda x}\left(1 - e^{-\lambda x}\right)^{\alpha\gamma-1} e^{-\left(\left(1-e^{-\lambda x}\right)^{\alpha}\right)^{\gamma}}}{1 - e^{-1}}. \tag{6}$$

Theorem 1. *Validity of the PDF of the Proposed Distribution*

Let $X > 0$, and let the PDF be defined as follows:

$$f(x;\lambda,\alpha,\gamma) = \frac{\gamma\alpha\lambda e^{-\lambda x}\left(1 - e^{-\lambda x}\right)^{\alpha-1}\left(\left(1 - e^{-\lambda x}\right)^{\alpha}\right)^{\gamma-1} e^{-\left(\left(1-e^{-\lambda x}\right)^{\alpha}\right)^{\gamma}}}{1 - e^{-1}}, \tag{7}$$

where $\lambda > 0$, $\alpha > 0$, $\gamma > 0$ are distribution parameters.

Then, $f(x;\lambda,\alpha,\gamma)$ is a valid PDF, i.e.:

i. $f(x;\lambda,\alpha,\gamma) \geq 0$, for all x

ii. $\int_0^{\infty} f(x;\lambda,\alpha,\gamma)dx = 1$

Proof 1.

i. Non-negativity: All the terms in the expression are non-negative for $x > 0$, because

$$\lambda > 0, \alpha > 0, \gamma > 0. \tag{8}$$

So, $f(x;\lambda,\alpha,\gamma) \geq 0$, for all x

ii. $\int_0^{\infty} f(x;\lambda,\alpha,\gamma)dx = \int_0^{\infty}\{(\gamma\alpha\lambda e^{-\lambda x}\ (1 - e^{-\lambda x})^{\alpha-1}\ ((1 - e^{-\lambda x})^{\alpha})^{\gamma-1} e^{-((1-e^{-\lambda x})^{\alpha})^{\gamma}})/(1 - e^{-1})\}dx.$ □

Make the substitution: $u = 1 - e^{-\lambda x} \implies x = -(1/\lambda)\ln(1-u)$

Then, $dx = (1/\lambda(1-u))du$.

Change of variable in the integral: $\int_0^{\infty} f(x;\lambda,\alpha,\gamma)dx = \int_0^1((\gamma\alpha u^{\alpha\gamma-1}e^{-u^{\alpha\gamma}})/(1 - e^{-1}))\ du = ((\gamma\alpha)/(1 - e^{-1}))\int_0^1 u^{\alpha\gamma-1}e^{-u^{\alpha\gamma}}du$

Let $z = u^{\alpha\gamma} \implies dz = \alpha\gamma u^{\alpha\gamma-1}du$.

Rewrite the integral: $(\gamma\alpha)/(1-e^{-1})\int_0^1 u^{\alpha\gamma-1}\ e^{-u^{\alpha\gamma}}du = ((\gamma\alpha)/(1-e^{-1}))\ \int_0^1((e^{-z}dz)/(\gamma\alpha)) = (1/(1-e^{-1}))\ \int_0^1 e^{-z}dz = (1-e^{-1})/(1-e^{-1}) = 1$.

Hence, $f(x;\lambda,\alpha,\gamma)$ is a valid PDF.

2.2. Survival and Hazard Functions. The survival function $S(x;\lambda,\alpha,\gamma)$ and hazard rate function $h(x;\lambda,\alpha,\gamma)$ are essential for survival and reliability analysis.

Survival function: $S(x;\lambda,\alpha,\gamma) = 1 - F(x;\lambda,\alpha,\gamma,)$

$$S(x;\lambda,\alpha,\gamma) = \frac{e^{-\left(\left(1-e^{-\lambda x}\right)^{\alpha}\right)^{\gamma}} - e^{-1}}{1-e^{-1}}. \tag{9}$$

Hazard function: $h(x;\lambda,\alpha,\gamma) = f(x;\lambda,\alpha,\gamma)/S(x;\lambda,\alpha,\gamma)$

$$h(x;\lambda,\alpha,\gamma) = \frac{\gamma\alpha\lambda e^{-\lambda x}\left(1-e^{-\lambda x}\right)^{\gamma\alpha-1} e^{-\left(\left(1-e^{-\lambda x}\right)^{\alpha}\right)^{\gamma}}}{e^{-\left(\left(1-e^{-\lambda x}\right)^{\alpha}\right)^{\gamma}} - \quad e^{-1}}. \tag{10}$$

2.3. Plot of the MFrEE Distribution. To illustrate the flexibility of the MFrEE distribution, we present plots of the PDF and CDF for selected parameter values. Figures 1, 2, 3, 4, 5, 6, 7, and 8 display the shapes of the PDF, CDF, survival, and hazard, respectively, under different choices of the shape and scale parameters.

Figure 1 displays plots of the PDF of the new MFrEE distribution for different values of γ, with $\lambda = 2$ and $\alpha = 3$. It is clear that the PDF of the MFrEE is unimodal and right-skewed. The modal value decreases as the values of γ increase, and the location of the mode also shifts.

Figure 2 shows the PDF for the same γ values as Figure 1, with $\lambda = 2$ and $\alpha = 10$. The PDF is unimodal and right-skewed. As γ increases, the modal value decreases, indicating that a smaller γ is better suited for data with a larger mode. The distribution's location also shifts with changes in α.

Figures 3 and 4 show the CDF plots of the MFrEE distribution. The CDFs all converge to 1.0. As the value of the parameter γ decreases (with other parameters fixed), the rate of convergence or growth rate of the CDF increases.

Figures 5 and 6 illustrate the survival function of the proposed distribution. As expected for lifetime data, the curves decrease as x increases, indicating the diminishing probability of survival over time. However, the rate at which the survival probability declines varies noticeably across parameter settings. This variation reflects the flexibility of the new distribution: It can capture slow, moderate, or rapid decay in survival probability. Such adaptability is crucial in practical applications where different underlying risk patterns such as early failures, constant risks, or long-tail survival must be accurately represented.

Figures 7 and 8 demonstrate that the new hazard function shows very interesting shapes, exhibiting two distinct behaviors in contrast to the only strictly increasing property of the base hazard function. The two figures illustrate how the shape parameter γ (gamma) fundamentally controls the behavior of the hazard function, which represents the instantaneous risk of failure over time (x).

For $\gamma < 1$: The hazard function is decreasing (DFR). This indicates where the risk of failure is highest initially and decreases over time as defective items fail early. For $\gamma = 1$: The hazard function is constant (CFR). This is the classic memoryless property of the exponential distribution, where the risk of failure is random and does not depend on any variables. For $\gamma > 1$, the hazard function is increasing (IFR). This models where the risk of failure increases as the item any variables.

Therefore, MFrEE distribution is highly flexible because its hazard function can simulate the entire bathtub curve commonly seen in reliability. This makes it a powerful tool for modeling a wide range of real-world failure processes and an excellent candidate for analyzing complex time-to-failure data in fields like engineering, medicine, and finance. By estimating the parameter γ, the model can be tailored to specific failure mechanisms.

2.4. Quantile Function of MFrEE Distribution. To derive the *quantile function* of your *new distribution,* we need to *invert the CDF.*

Given CDF

$$F(x;\lambda,\alpha,\gamma) = \frac{e^{-\left(\left(1-e^{-\lambda x}\right)^{\alpha}\right)^{\gamma}} - 1}{e^{-1} - 1}, \quad x > 0. \tag{11}$$

Let u = $F(x;\lambda,\alpha,\gamma)$. Then, $u = (e^{-((1-e^{-\lambda x})^{\alpha})^{\gamma}} - 1)/(e^{-1} - 1)$.

Multiply both sides by $e^{-1} - 1$:

$$u\left(e^{-1}-1\right) = e^{-\left(\left(1-e^{-\lambda x}\right)^{\alpha}\right)^{\gamma}} - 1. \tag{12}$$

Add 1 to both sides:

$$u\left(e^{-1}-1\right) + 1 = e^{-\left(\left(1-e^{-\lambda x}\right)^{\alpha}\right)^{\gamma}}. \tag{13}$$

Take the natural logarithm:

$$\ln\left(u\left(e^{-1}-1\right)+1\right) = -\left(\left(1-e^{-\lambda x}\right)^{\alpha}\right)^{\gamma}. \tag{14}$$

Finally, solve for x: $x = -(1/\lambda)\ln\ (1 - [-\ln\ (u\ (e^{-1} - 1) + 1)]^{(1/\alpha\gamma)})$.

Quantile function:

$$Q(u) = -\frac{1}{\lambda}\ln\left(1 - \left[-\ln\left(u\left(e^{-1}-1\right)+1\right)\right]^{(1/(\alpha\gamma))}\right), \quad 0 < u < 1. \tag{15}$$

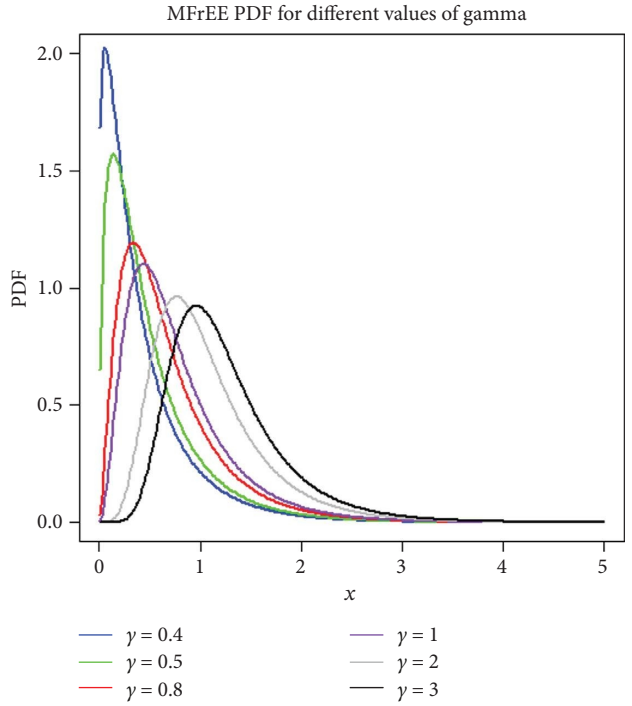

FIGURE 1: Plots of the probability density function (PDF) of the MFrEE distribution for different values of the shape parameter $\gamma \in \{0.4, 0.5, 0.8, 1, 2, 3\}$ while keeping $\lambda = 2$, and $\alpha = 3$ fixed. The figure highlights how changes in the shape parameter affect the skewness and peak behavior of the density function.

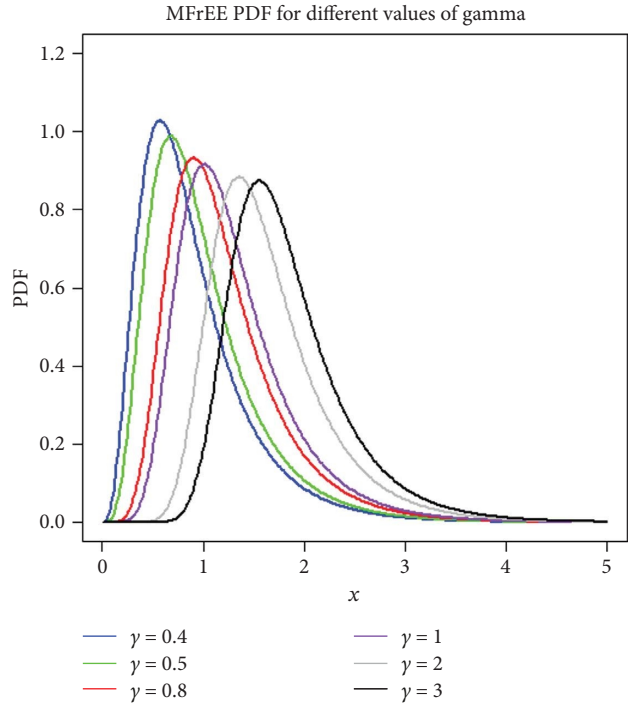

FIGURE 2: Plots of the probability density function (PDF) of the MFrEE distribution for different values of the shape parameter $\gamma \in \{0.4, 0.5, 0.8, 1, 2, 3\}$ while keeping $\lambda = 2$, $\alpha = 10$ fixed.

When $u = 0.5$, the quantile function gives the median of the MFrEE distribution.

2.5. Mean and Moments of the MFrEE Distribution. Let us go step by step using the PDF of the *MFrEE* distribution.

The PDF is given by

$$f(;,\lambda,\alpha,\gamma) = \frac{\gamma\alpha\lambda e^{-\lambda x}\left(1-e^{-\lambda x}\right)^{\alpha-1}\left(\left(1-e^{-\lambda x}\right)^{\alpha}\right)^{\gamma-1}e^{-\left(\left(1-e^{-\lambda x}\right)^{\alpha}\right)^{\gamma}}}{1-e^{-1}}. \tag{16}$$

This simplifies to:

$$f(x;\lambda,\alpha,\gamma) = \frac{\gamma\alpha\lambda e^{-\lambda x}\left(1-e^{-\lambda x}\right)^{\alpha\gamma-1}e^{-\left(\left(1-e^{-\lambda x}\right)^{\alpha}\right)^{\gamma}}}{1-e^{-1}}. \tag{17}$$

We want to compute the rth moment: $\mu_r{}' = E(X^r)$

$$\mu_r{}' = \int_0^{\infty} x^r f(x)dx. \tag{18}$$

Let us simplify this using the substitution:
Let $u = 1 - e^{-\lambda x} \Longrightarrow \quad x = -(1/\lambda)\ln\ (1-u)$.
Then, $dx = (1/\lambda(1-u))du$.
Also, $e^{-\lambda x} = 1 - u$.
Now rewrite the rth moment:

$$\begin{aligned}\mu_r{}' &= \int_0^1 \left(-\frac{1}{\lambda}\ln\ (1-u)\right)^r \frac{\alpha\gamma\lambda(1-u).u^{\alpha\gamma-1}e^{-u^{\alpha\gamma}}}{1-e^{-1}} \cdot \quad \frac{1}{\lambda(1-u)}du \\ &= \frac{\alpha\gamma}{\left(1-e^{-1}\right)\lambda^r}\int_0^1 \left(\ln\left(\frac{1}{1-u}\right)\right)^r \cdot u^{\alpha\gamma-1}e^{-u^{\alpha\gamma}}du.\end{aligned} \tag{19}$$

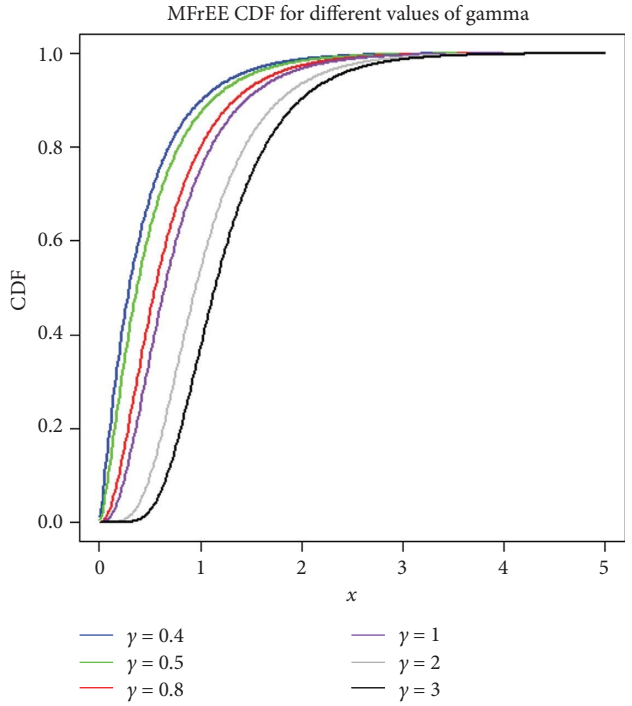

Figure 3: Plots of CDF with different values of parameter $\gamma \in \{0.4, 0.5, 0.8, 1, 2, 3\}$ while keeping $\lambda = 2$, $\alpha = 3$ fixed.

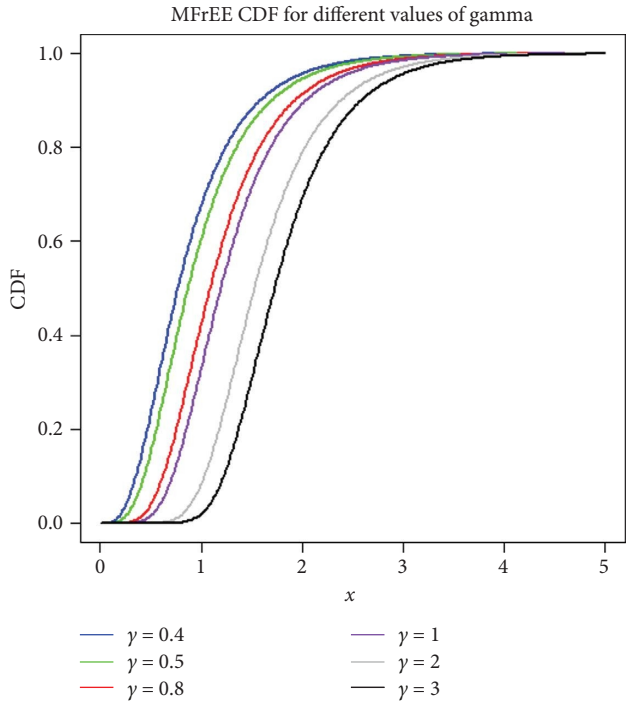

Figure 4: Plots of CDF with different values of parameter $\gamma \in \{0.4, 0.5, 0.8, 1, 2, 3\}$ while keeping $\lambda = 2$, $\alpha = 10$ fixed.

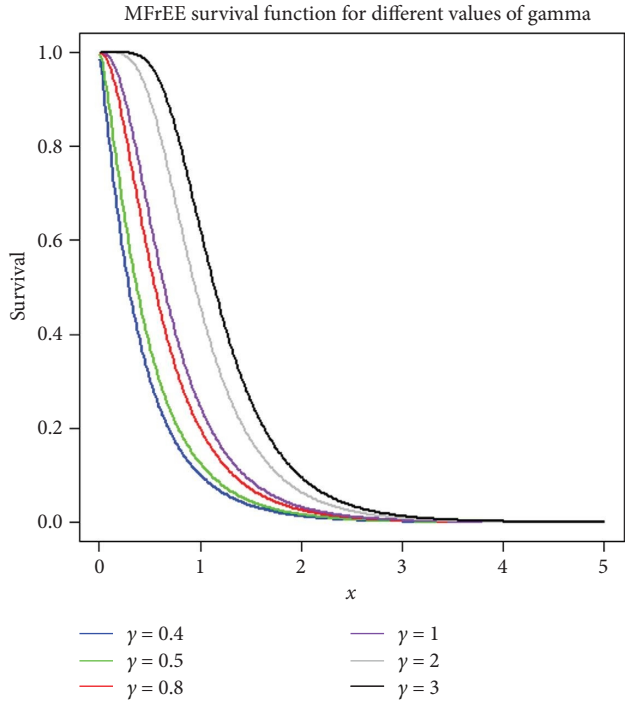

Figure 5: Plots of survival function with $\gamma \in \{0.4, 0.5, 0.8, 1, 2, 3\}$ while keeping $\lambda = 2$, $\alpha = 3$ fixed.

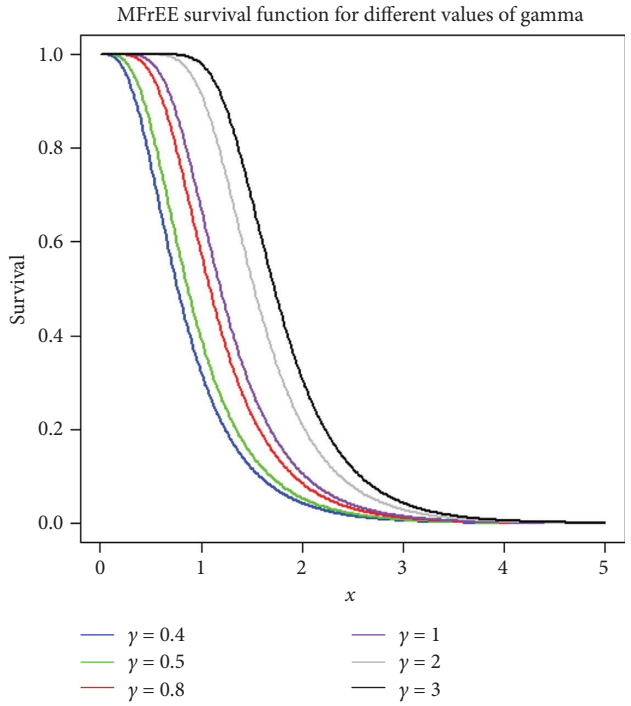

Figure 6: Plots of survival function with parameter $\gamma \in \{0.4, 0.5, 0.8, 1, 2, 3\}$ while keeping $\lambda = 2$, $\alpha = 10$ fixed.

Now, to evaluate the moment, expand $(\ln(1/(1-u)))^r$ using a *power series*.

Power series of $\ln(1/(1-u)) = \sum_{n=1}^{\infty} u^n/n$

$$\text{So, } \ln\left(\frac{1}{1-u}\right)^r = \left(\sum_{n=1}^{\infty} \frac{u^n}{n}\right)^r = \sum_{n=r}^{\infty} A_{n,r} u^n, \tag{20}$$

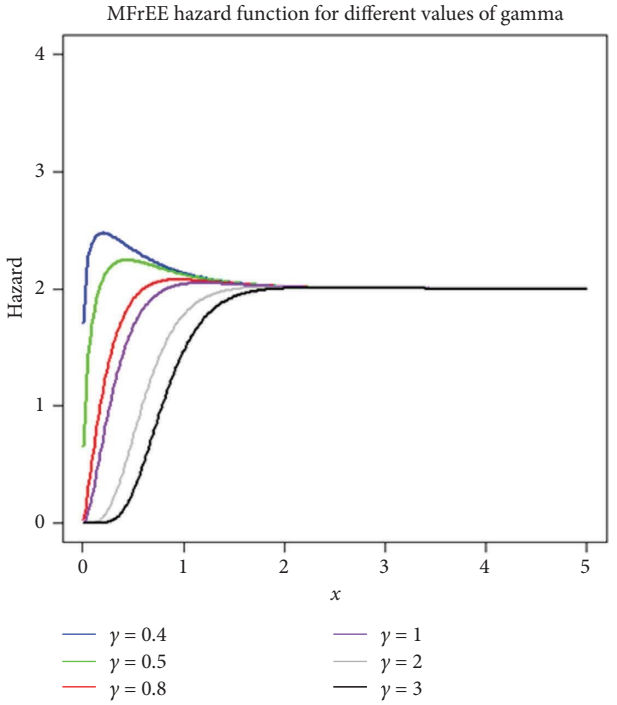

FIGURE 7: Plots of hazard function with parameter $\gamma \in \{0.4, 0.5, 0.8, 1, 2, 3\}$ while keeping $\lambda = 2$, $\alpha = 3$ fixed.

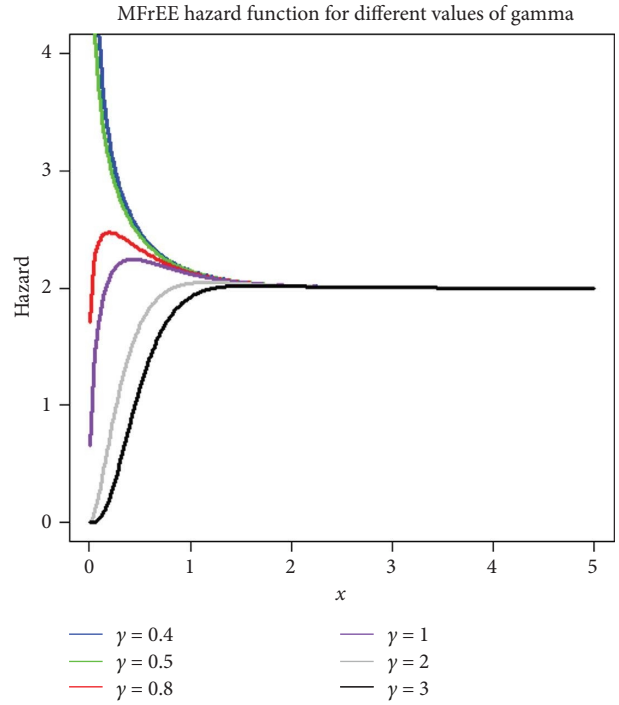

FIGURE 8: Plots of hazard function with parameter $\gamma \in \{0.4, 0.5, 0.8, 1, 2, 3\}$ while keeping $\lambda = 2$, $\alpha = 1.5$ fixed.

where $A_{n,r}$ are coefficients from the rth power of the series. They can be expressed using multinomial expansions, or more simply for small r using the convolution of the series.

So, we get the following equation:

$$\mu_r' = \frac{\alpha\gamma}{\left(1-e^{-1}\right)\lambda^r}\int_0^1\left(\sum_{n=r}^{\infty}A_{n,r}u^n\right).u^{\alpha\gamma-1}e^{-u^{\alpha\gamma}}du = \frac{\alpha\gamma}{\left(1-e^{-1}\right)\lambda^r}\sum_{n=r}^{\infty}A_{n,r}\int_0^1 u^{n+\alpha\gamma-1}e^{-u^{\alpha\gamma}}du. \tag{21}$$

Now substitute $z = u^{\alpha\gamma} \Longrightarrow u = z^{(1/\alpha\gamma)} \Longrightarrow du = (1/(\alpha\gamma))z^{1/(\alpha\gamma)-1}dz$.

The integral becomes $\int_0^1 u^{n+\alpha\gamma-1}\, e^{-u^{\alpha\gamma}}du = (1/(\alpha\gamma))\int_0^1 z^{(n/\alpha\gamma)}e^{-z}dz = (1/(\alpha\gamma))\Gamma(1+(n/(\alpha\gamma)),\, 1)$.

Hence, the final rth moment is given by the following equation:

$$\mu_r' = \frac{1}{\left(1-e^{-1}\right)\lambda^r}\sum_{n=r}^{\infty}A_{n,r}\Gamma\left(1+\frac{n}{\alpha\gamma},\, 1\right). \tag{22}$$

Final expression for the mean is as follows:

$$\mu_1' = \frac{1}{\left(1-e^{-1}\right)\lambda^1}\sum_{n=1}^{\infty}\frac{1}{n}\quad\Gamma\left(1+\frac{n}{\alpha\gamma},\, 1\right). \tag{23}$$

Now, for the *second moment*, $r = 2$:

$$\mu_2' = \frac{1}{\left(1-e^{-1}\right)\lambda^2}\sum_{n=2}^{\infty}A_{n,2}\quad\Gamma\left(1+\frac{n}{\alpha\gamma},\, 1\right). \tag{24}$$

Variance: The variance of the *MFrEE* distribution using first and second moments is as follows:

$$\mathrm{Var}(x) = \mu_2' - (\mu_1')^2. \tag{25}$$

2.6. Moment-Generating Function (MGF). To derive the MGF of the distribution with the simplified PDF:

$$f(x;\lambda,\alpha,\gamma) = \frac{\gamma\alpha\lambda e^{-\lambda x}\left(1-e^{-\lambda x}\right)^{\alpha\gamma-1}e^{-\left(\left(1-e^{-\lambda x}\right)^{\alpha}\right)^{\gamma}}}{1-e^{-1}}. \tag{26}$$

We define MGF as follows: $M_X(t) = E(e^{tX}) = \int_0^{\infty}e^{tX}f(x)dx$.

Using the *Taylor expansion* for the exponential in the definition of MGF as follows:

$$M_X(t) = E\left(e^{tX}\right) = \sum_{r=0}^{\infty}\frac{t^r}{r!}\mu_r', \tag{27}$$

$$M_X(t) = \sum_{r=0}^{\infty}\frac{t^r}{r!\left(1-e^{-1}\right)\lambda^r}\sum_{n=r}^{\infty}A_{n,r}\Gamma\left(1+\frac{n}{\alpha\gamma},\, 1\right). \tag{28}$$

2.7. Maximum Likelihood Estimation (MLE) Method. To estimate the parameters of the MFrEE distribution using the MLE method, we follow a standard procedure.

We are given the PDF as follows:

$$f(x;\lambda,\alpha,\gamma) = \frac{\gamma\alpha\lambda e^{-\lambda x}\left(1-e^{-\lambda x}\right)^{\alpha\gamma-1}e^{-\left(\left(1-e^{-\lambda x}\right)^{\alpha}\right)^{\gamma}}}{1-e^{-1}}. \tag{29}$$

Suppose you have a random sample $x_1, x_2, \ldots, x_n$ from this distribution. The *likelihood function* is as follows:

$$L(\lambda, \alpha, \gamma) = \prod_{i=1}^{n} f(x_i; \lambda, \alpha, \gamma),$$
$$\text{So, } L(\lambda, \alpha, \gamma) = \left(\frac{\gamma\alpha\lambda}{1 - e^{-1}}\right)^n \prod_{i=1}^{n} \left(1 - e^{-\lambda x_i}\right)^{\alpha\gamma - 1} e^{-\lambda x_i - \left(\left(1 - e^{-\lambda x_i}\right)^{\alpha}\right)^{\gamma}}. \tag{30}$$

Take the log of the likelihood as follows:

$$l(\lambda, \alpha, \gamma) = n\log(\gamma\alpha\lambda) - n\log\left(1 - e^{-1}\right) + (\alpha\gamma - 1)\sum_{i=1}^{n}\log\left(1 - e^{-\lambda x_i}\right) - \lambda\sum_{i=1}^{n} x_i - \sum_{i=1}^{n}\left(1 - e^{-\lambda x_i}\right)^{\alpha\gamma}. \tag{31}$$

We obtain the MLEs by solving the system: $(\partial l)/(\partial\alpha) = 0$, $((\partial l)/(\partial\gamma)) = 0$, $((\partial l)/(\partial\lambda)) = 0$.

Hence,

$$\frac{\partial l}{\partial \alpha} = \frac{n}{\alpha} + \gamma\sum_{i=1}^{n}\log\left(1 - e^{-\lambda x_i}\right) - \gamma\sum_{i=1}^{n}\left(1 - e^{-\lambda x_i}\right)^{\alpha\gamma}\log\left(1 - e^{-\lambda x_i}\right), \tag{32}$$

$$\frac{\partial l}{\partial \gamma} = \frac{n}{\gamma} + \alpha\sum_{i=1}^{n}\log\left(1 - e^{-\lambda x_i}\right) - \alpha\sum_{i=1}^{n}\left(1 - e^{-\lambda x_i}\right)^{\alpha\gamma}\log\left(1 - e^{-\lambda x_i}\right), \tag{33}$$

$$\frac{\partial l}{\partial \lambda} = \frac{n}{\lambda} - \sum_{i=1}^{n} x_i + (\alpha\gamma - 1)\sum_{i=1}^{n}\frac{x_i e^{-\lambda x_i}}{1 - e^{-\lambda x_i}} - \sum_{i=1}^{n}\left(1 - e^{-\lambda x_i}\right)^{\alpha\gamma - 1} \cdot \alpha\gamma x_i e^{-\lambda x_i}. \tag{34}$$

The MLEs of the parameters of the proposed distribution do not have closed-form (analytical) solutions due to the complexity of the likelihood equations. Therefore, the MLEs must be obtained using *numerical optimization techniques*, such as the *Newton–Raphson method, expectation–maximization (EM)* algorithm, or other iterative numerical procedures.

Since the score function defined in equations (13)–(15) cannot be solved in closed form, numerical methods can be employed to estimate the parameters. Now, the *Hessian matrix* is the 3×3 *matrix of second-order partial derivatives*:

$$H(\theta) = \begin{pmatrix} \frac{\partial^2 l}{\partial \alpha^2} & \frac{\partial^2 l}{\partial \alpha \partial \gamma} & \frac{\partial^2 l}{\partial \alpha \partial \lambda} \\ \frac{\partial^2 l}{\partial \gamma \partial \alpha} & \frac{\partial^2 l}{\partial \gamma^2} & \frac{\partial^2 l}{\partial \gamma \partial \lambda} \\ \frac{\partial^2 l}{\partial \lambda \partial \alpha} & \frac{\partial^2 l}{\partial \lambda \partial \gamma} & \frac{\partial^2 l}{\partial \lambda^2} \end{pmatrix}. \tag{35}$$

The observed information matrix is as follows: $I(\theta) = -H(\theta)$, where $\theta = (\lambda, \alpha, \gamma)^T$.

The *variance–covariance matrix of the MLEs* is given by the inverse as follows:

$$\widehat{\text{Var}}(\widehat{\theta}) = I(\theta)^{-1}. \tag{36}$$

This matrix provides the standard errors (SEs) for $\widehat{\alpha}, \widehat{\gamma}, \widehat{\lambda}$, which are crucial for inference.

2.7.1. Asymptotic Distribution of MLEs. The MLEs are random variables that depend on the sample. Under standard regularity *conditions*, MLEs are *consistent*, *asymptotically normal*, and *asymptotically efficient* [42–44].

Thus, the MLEs satisfy

$$\sqrt[n]{n}(\widehat{\theta} - \theta) \xrightarrow{d} N\left(0, I(\theta)^{-1}\right), \tag{37}$$

where $\widehat{\theta} = (\widehat{\alpha}, \widehat{\gamma}, \widehat{\lambda})^T$ denotes the vector of MLEs and $I(\theta)$ is the Fisher information matrix. This result implies that, for large samples, the MLEs are approximately normally distributed with mean equal to the true parameter values and

covariance matrix given by the inverse of the Fisher information.

Hence, the *asymptotic confidence interval (CI)* for each parameter θ_i can be constructed as follows:

$$\widehat{\theta}_i \pm Z_{(\beta/2)}\mathrm{SE}\left(\widehat{\theta}_i\right), \quad i = \lambda, \alpha, \gamma, \tag{38}$$

where $Z_{(\beta/2)}$ is the standard normal quantile corresponding to the significance level β and $\mathrm{SE}(\widehat{\theta}_i) = \sqrt{\widehat{\mathrm{var}}(\widehat{\theta}_i)}$ is the SE obtained from the inverse of the observed information matrix.

3. Results

3.1. Simulation Studies. To investigate the performance of the MLEs of the parameters of the proposed distribution, we conducted a simulation study. The simulation focused on assessing the estimators' accuracy and consistency by examining their *bias, mean squared error (MSE)*, and variability under varying sample sizes and parameter settings.

3.1.1. Inverse Transform Method. In this method, random samples were generated using the inverse of the CDF, provided the quantile function is available or can be approximated numerically.

Random samples from the MFrEE distribution were generated using the inverse transform method, based on the derived quantile function. This approach is appropriate because the quantile function is available in closed form (or can be evaluated numerically with high accuracy), allowing efficient generation of random observations. The simulation study was conducted for several sample sizes, specifically: $n = 10$, 50, 100, 150, 500, and 1000 to examine the performance of the estimators under both small- and large-sample conditions. These sample sizes are commonly used in simulation studies in reliability and survival modeling and represent realistic data situations encountered in practice. Each scenario was replicated a sufficiently large number of times to ensure stable estimates of bias, MSE, and CP; this number also balances precision with computational efficiency.

The simulation study was organized into two parts. First, we investigated the consistency of the MLEs of the parameters γ, α, λ. According to the definition of consistency, an estimator should converge to the true parameter value as the sample size increases, and the MSE should tend toward zero as $n \longrightarrow \infty$. To verify this, datasets were generated under the parameter settings specified in Tables 1 and 2, with sample size up to $n = 1000$. For each parameter configuration, we computed the sequence of MSE values as n increased. A decreasing trend in MSE indicates that the MLEs exhibit the desired consistency. Coverage probabilities were also examined, and they approached the nominal 95% level for large samples, demonstrating that the CIs are well-calibrated asymptotically. A 95% coverage level is adopted because it provides a widely accepted balance between precision and reliability (Tables 1 and 2).

All simulations were performed in R Version 4.2.1, using a fixed random seed to ensure reproducibility. Parameter estimation relied on numerical maximization of the log-likelihood function using the optim() function with the BFGS algorithm and computation times remained efficient across all parameter scenarios.

3.1.2. Acceptance–Rejection (AR) Method. The AR method was employed to generate random samples from the MFrEE distribution. Using the EED as the proposal allowed efficient sampling while preserving the key characteristics of the MFrEE distribution.

The AR algorithm was applied to conduct two simulation studies to investigate the effects of varying parameter values and sample sizes on the distribution's behavior. The results of these simulations are presented below in Figures 9 and 10.

Figure 9 confirms that the AR method effectively generates samples that reflect the theoretical sensitivity of the MFrEE distribution to changes in the shape parameter γ. This highlights the model's adaptability for applications where tail behavior plays a critical role.

When $\gamma = 0.5$, the simulated data show a concentration around smaller values, with the histogram aligning closely with the lighter-tailed theoretical PDF. The distribution exhibits reduced variability, confirming that smaller γ values produce lighter tails and a more concentrated failure-time pattern. This implies a relatively lower probability of extreme or unusually large observations.

For $\gamma = 2$, the histogram displays a much wider spread, and the overlay reveals that the sample more frequently generates large values, corresponding to a heavier right tail. This demonstrates that increasing γ significantly enhances the tail thickness and alters the distribution's skewness. As a result, the MFrEE distribution becomes more capable of modeling extreme lifetimes and high-variability failure mechanisms.

The close agreement between the histograms and the theoretical PDFs in both panels confirms the accuracy of the AR sampling method. Moreover, these plots highlight the essential role of the parameter γ in shaping the distribution—from light-tailed to heavy-tailed behavior—thereby illustrating the flexibility of the MFrEE model for reliability and survival applications (Figure 10).

3.2. Application to Real Data. The performance of the new proposed MFrEE which has three parameters is compared with three current models using three real-world datasets: EED [2], alpha power transformed exponentiated exponential distribution (APTEE) [33], two-parameter Weibull distribution, and exponential distribution. EED is the base distribution from which we derived the new model and is used as a reference for performance comparisons of the model.

The other models are well known in literature, and we need to fit them for comparison. Akaike information criterion (AIC), Bayesian information criterion (BIC), corrected Akaike information criterion (AICc), and Kolmogorov–Smirnov goodness-of-fit test (KS) are the criteria used to compare the performance of our model with the other models. As far as the given data are concerned, the

Table 1: Summary of MSE for different samples for true parameters ($\lambda = 2, \alpha = 1.5, \gamma = 1.3$).

n	MLE			Bias			MSE			Coverage probability (CP)		
	$\hat{\lambda}$	$\hat{\alpha}$	$\hat{\gamma}$	$\hat{\lambda}$	$\hat{\alpha}$	$\hat{\gamma}$	$\hat{\lambda}$	$\hat{\alpha}$	$\hat{\gamma}$	$\hat{\lambda}$	$\hat{\alpha}$	$\hat{\gamma}$
10	3.8726	1.959	1.5676	0.8553	0.1889	0.1162	2.9208	0.1587	0.0601	0.9120	0.906	0.924
50	2.1799	1.6552	1.3241	0.1005	0.0198	0.0122	0.1872	0.0116	0.0044	0.9253	0.911	0.938
100	2.597	1.800	1.4406	0.0443	0.0148	0.0091	0.0971	0.0080	0.0030	0.9452	0.953	0.942
150	2.2732	1.6616	1.3292	0.0231	0.0088	0.0054	0.0561	0.0043	0.0016	0.9492	0.956	0.952
300	2.407	1.6608	1.3287	0.0112	0.0039	0.0024	0.0300	0.0020	0.0007	0.9501	0.955	0.957
500	1.9167	1.5162	1.2129	0.0005	0.0002	0.0009	0.0185	0.0012	0.0005	0.9502	0.955	0.958
1000	1.9527	1.4331	1.2865	0.0012	0.0005	0.0003	0.0069	0.0006	0.0002	0.9501	0.955	0.958

Table 2: Summary of MSE for different samples for true parameters ($\lambda = 2, \alpha = 3, \gamma = 3$).

n	MLE			Bias			MSE			Coverage probability (CP)		
	$\hat{\lambda}$	$\hat{\alpha}$	$\hat{\gamma}$	$\hat{\lambda}$	$\hat{\alpha}$	$\hat{\gamma}$	$\hat{\lambda}$	$\hat{\alpha}$	$\hat{\gamma}$	$\hat{\lambda}$	$\hat{\alpha}$	$\hat{\gamma}$
10	1.8939	3.6513	3.5631	0.8553	0.1889	0.1162	2.9208	0.1587	0.0601	0.9354	0.921	0.915
50	2.1051	3.3546	3.4642	0.1005	0.0198	0.0122	0.1872	0.0116	0.0044	0.9391	0.93	0.928
100	2.3103	3.6947	3.3798	0.0443	0.0148	0.0091	0.0971	0.0080	0.0030	0.945	0.945	0.942
150	2.2131	3.4808	3.3834	0.0232	0.0088	0.0054	0.0561	0.0043	0.0016	0.9483	0.956	0.951
300	2.3327	3.5856	3.2564	0.0112	0.0039	0.0024	0.0300	0.0020	0.0007	0.9512	0.9503	0.952
500	2.1369	3.2462	3.1952	0.0005	0.0002	0.0009	0.0185	0.0012	0.0005	0.9503	0.953	0.955
1000	2.0116	3.0316	3.0572	0.0012	0.0005	0.0003	0.0069	0.0006	0.0002	0.9510	0.961	0.957

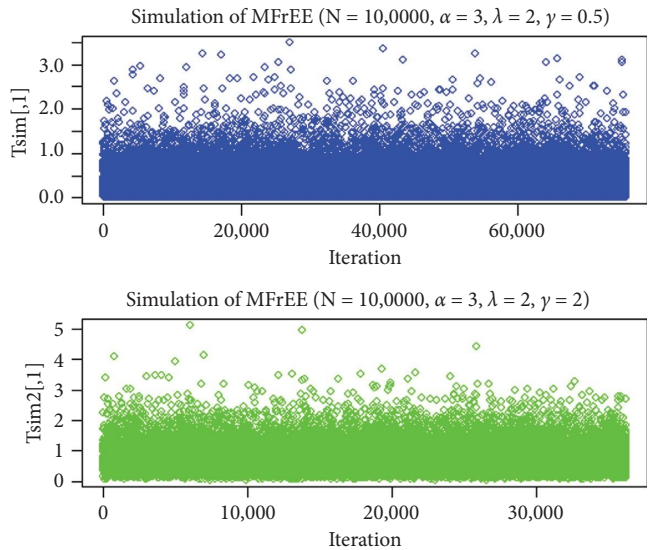

Figure 9: Two realizations of the simulation from the new distribution given values of the parameters $\alpha = 3$, $\lambda = 2$ with $\gamma = 0.5$ (top plot) and $\gamma = 2$ (bottom plot).

best model is the distribution with the lowest values of AIC, BIC, and AICc, or the maximum p-value for the KS test. Results of analysis are displayed in Tables 1, 2, 3, 4, 5, and 6.

Datasets. Three real-world datasets were employed in this study to illustrate the applicability and fitting performance of the proposed distributions.

3.2.1. Dataset 1: Pharmacokinetics of Indomethacin. The first dataset is the Pharmacokinetics of Indomethacin (the Indometh data frame has 66 rows and 3 columns of data on the pharmacokinetics of Indomethacin), and data are taken from a website (https://mtweb.cs.ucl.ac.uk/mus/bin/install_R/R-3.1.1/src/library/datasets/man/Indometh.Rd).

Histogram of the data is given in Figure 11. Results of data fitting are given in Tables 3 and 4. The new model has got lower values for the goodness-of-fit statistics. Table 4 presents the values of several model selection and goodness-of-fit criteria for the competing lifetime distributions fitted to the indomethacin dataset. Across the different information criteria (AIC, CAIC, BIC, and HQIC), the MFrEE distribution consistently attains the smallest values (AIC = 66.81, CAIC = 66.99, BIC = 71.18, HQIC = 68.53).

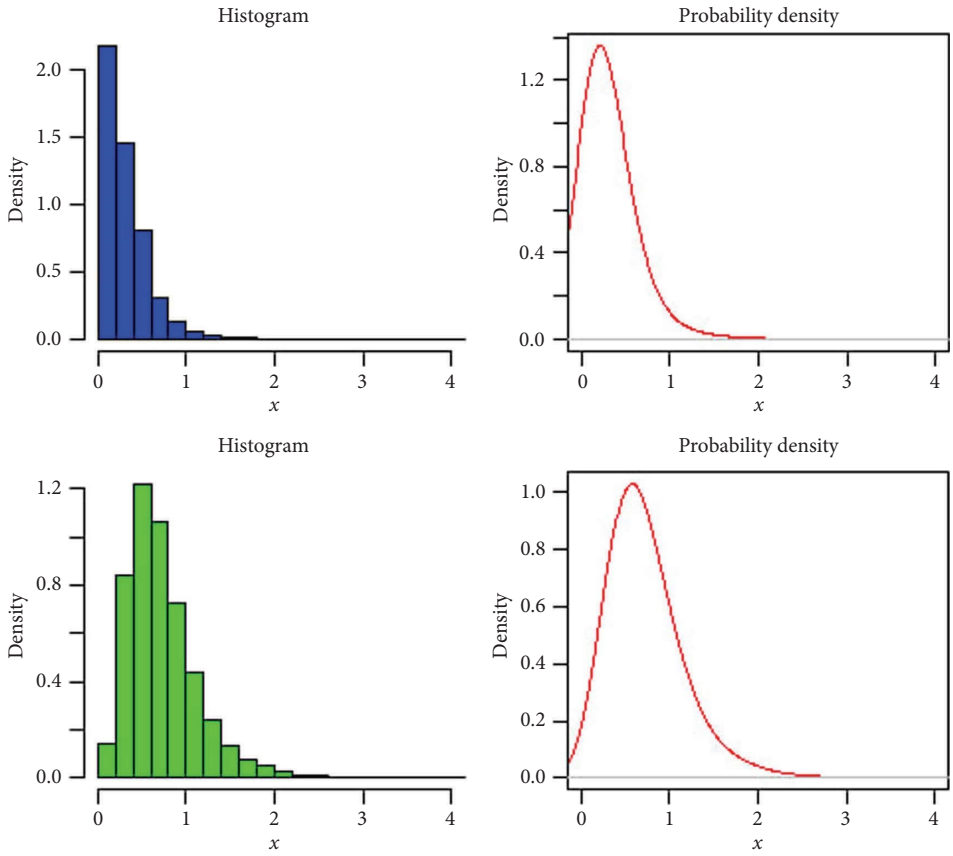

FIGURE 10: Histograms of the new distribution given values of the parameters $\alpha = 3$, $\lambda = 2$ with $\gamma = 0.5$ (top plot) and $\gamma = 2$ (bottom plot). Each subplot displays the random sample and the corresponding histogram overlaid with the theoretical probability density function (PDF).

Lower values of these criteria indicate better model performance by balancing goodness of fit with model complexity. Therefore, the MFrEE model provides the most efficient and parsimonious representation of the data among all models considered.

Regarding the KS goodness-of-fit statistics, the MFrEE model also yields the smallest KS value (31.40) and the largest p-value (0.125) compared with the competing models. A larger KS p-value (greater than the significance level $\alpha = 0.05$) indicates that there is no statistical evidence to reject the hypothesis that the MFrEE model fits the data well. Although all models have p-values above 0.10 and therefore provide acceptable fits, the MFrEE distribution demonstrates comparatively better agreement with the empirical data.

Overall, based on both the information criteria and the KS goodness-of-fit results, the MFrEE distribution is identified as the best-fitting model for the indomethacin dataset.

3.2.2. Dataset 2: Data on Kidney Infection of 38 Patients. The second datasets were obtained from McGilchrist C. and Aisbett C. [45], which reports frailty values estimated from a study investigating the recurrence times of infections in 38 patients undergoing kidney dialysis. The dataset captures individual-specific unobserved heterogeneity (frailty terms) that influence the recurrence process, making it particularly suitable for evaluating flexible lifetime models. The second dataset used in this study is the repair time dataset, which comprises 30 observations representing the time between failures (measured in hours or a consistent time unit) of a set of repairable units. This dataset was originally reported by Murthy et al. [46] and is widely used in reliability analysis literature as a benchmark for evaluating lifetime distributions:

0.2, 0.2, 0.4, 0.4, 0.4, 0.4, 0.4, 0.4, 0.5, 0.5, 0.5, 0.5, 0.5, 0.5, 0.5, 0.5, 0.6, 0.6, 0.6, 0.6, 0.7, 0.7, 0.7, 0.7, 0.7, 0.7, 0.7, 0.7, 0.8, 0.8, 0.8, 0.8, 1.0, 1.0, 1.1, 1.1, 1.1, 1.1, 1.1, 1.1, 1.2, 1.2, 1.2, 1.2, 1.2, 1.2, 1.3, 1.3, 1.3, 1.3, 1.4, 1.4, 1.5, 1.5, 1.5, 1.5, 1.5, 1.5, 1.7, 1.7, 1.7, 1.7, 1.8, 1.8, 1.9, 1.9, 2.1, 2.1, 2.2, 2.2, 2.3, 2.3, 2.9, 2.9, 3.0, 3.0.

(39)

Table 3: Estimates of fitted distributions for indomethacin data.

Model	$\widehat{\alpha}$	$\widehat{\lambda}$	$\widehat{\gamma}$
EED (base)	0.9547063	1.6085653	
MFrEE	2.4704280	3.2697413	0.5497995
APTEE	0.9990543	0.1760800	4.1498528
Weibull	1.249307	3.735040	
Exponential		1.689705	

Table 4: Model comparison criteria for indomethacin data.

Model	AIC	CAIC	BIC	HQIC	KS value	p-value
EED	70.89	71.28	77.46	73.49	32.45	0.103
MFrEE	66.81	66.99	71.18	68.53	31.40	0.125
APTEE	76.42	76.81	82.98	79.01	35.2	0.106
Weibull	76.61	76.79	80.98	88.34	41.30	0.109
Exponential	69.76	69.82	69.95	69.63	41.38	0.108

Table 5: Estimates of fitted distributions for kidney data.

Model	$\widehat{\alpha}$	$\widehat{\lambda}$	$\widehat{\gamma}$
EED (base)	1.663843	3.539909	
MFrEE	1.150866	2.623059	4.816219
APTEE	0.9996383	0.3377899	5.7879719
Exponential		0.844444	

The parameter estimations are displayed in Table 5. Based on the goodness-of-fit statistics of the patients undergoing kidney data, the histogram and plots of the predicted densities for the four most competitive probability distributions are displayed in Figure 12. These graphs match the results shown in Table 6.

Table 6 provides the results of several model selection and goodness-of-fit criteria used to compare candidate lifetime distributions for the kidney dataset. Across all information criteria—AIC, CAIC, BIC, and HQIC—the MFrEE distribution achieves the lowest values (AIC = 143.97, CAIC = 144.14, BIC = 148.63, HQIC = 145.83). These lower values indicate that the MFrEE model offers the best balance between goodness of fit and model complexity. Thus, based on information criteria alone, the MFrEE distribution is the most efficient and parsimonious model for this dataset.

The KS goodness-of-fit results further reinforce this conclusion. The MFrEE model yields the smallest KS statistic (69.98) and the highest p-value (0.4038) among all competing distributions. Importantly, this p-value is substantially higher than the conventional significance level ($\alpha = 0.05$), indicating strong evidence that the MFrEE model fits the empirical data well. In contrast, the baseline EED and exponential models exhibit very small p-values (0.0059 and 0.000), implying poor fit and clear rejection at $\alpha = 0.05$. The APTEE model shows marginal adequacy ($p = 0.057$), but still performs notably worse than the proposed MFrEE distribution.

Overall, both the information criteria and KS statistics consistently identify the MFrEE distribution as the best-fitting model for the kidney dataset, offering substantially improved fit relative to the existing alternatives.

3.2.3. Dataset 3: Fatality Rates of 106 Patients. The third datasets were used to evaluate the applicability of the proposed model. According to Cordero-Franco et al. [47], the dataset includes the fatality rates of 106 patients in Mexico during the COVID-19 pandemic, which lasted from March 4, 2020, to July 20, 2020. For convenience, the rates have been scaled by dividing them by five:

1.7652, 1.2210, 1.8782, 2.9942, 2.0766, 1.4534, 2.6440, 3.2996, 2.3330, 1.2030, 2.1710, 1.2244,
1.3312, 0.6880, 1.1708, 2.1370, 2.0070,
1.0484, 0.8668, 1.0286, 1.5260, 2.9208, 1.5806, 1.2740, 0.7074, 1.2654, 0.9460, 0.6430,
1.8568, 2.5756, 1.7626, 2.0086, 1.4520, 1.1970,
1.2824, 0.6790, 0.8848, 1.9870, 1.5680, 1.9100, 0.6998, 0.7502, 1.3936, 0.6572, 2.0316, 1.6216, 1.3394,
1.4302, 1.3120, 0.4154, 0.7556, 0.5976, 0.6672, 1.3628, 1.5708, 1.6650, 1.7120, 0.6456, (40)
1.4972, 1.3250, 1.2280, 0.9818, 0.9322, 1.0784, 2.4084,
1.7392, 0.3630, 0.6654, 1.0812, 1.2364, 0.2082, 0.3600, 0.9898, 0.8178, 0.6718, 0.4140, 0.6596, 1.0634, 1.0884,
0.9114, 0.8584, 0.5000, 1.3070, 0.9296, 0.9394, 1.0918, 0.8240, 0.7884, 0.6438, 0.2804,
0.4876, 0.6514, 0.7264, 0.6466, 0.6054, 0.4704, 0.2410, 0.6436, 0.5852, 0.5202,
0.4130, 0.6058, 0.4116, 0.4652, 0.5052, 0.3846.

Like the first and second datasets, MFrEE results show a better fit than other distributions that were taken into consideration in the third data sets. In all three datasets fitting cases, the new model performs better (Tables 7 and 8 and Figure 13).

Table 8 summarizes the performance of four competing lifetime distributions applied to the fatality rate dataset. Across all reported information criteria—AIC, CAIC, BIC, and HQIC—the MFrEE distribution consistently achieves the lowest values (AIC = 186.25, CAIC = 186.36,

Table 6: Model comparison criteria for kidney data.

Model	AIC	CAIC	BIC	HQIC	KS value	*p*-value
EED (base)	155.64	155.97	162.63	158.43	74.82	0.0059
MFrEE	143.97	144.14	148.63	145.83	69.98	0.4038
APTEE	160.26	160.59	167.25	163.05	77.13	0.057
Exponential	179.69	179.75	182.03	180.63	88.85	0.000

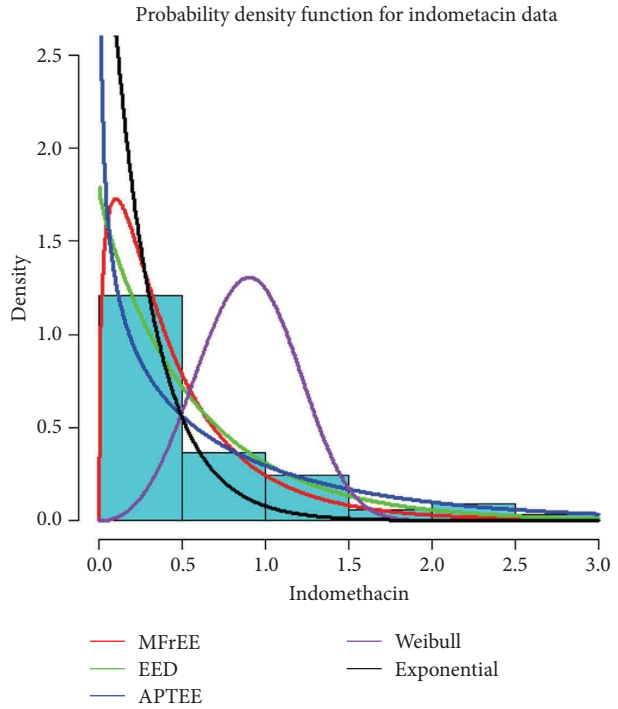

Figure 11: Plots for the fitted MFrEE pdf and other models to the Indomethacin data.

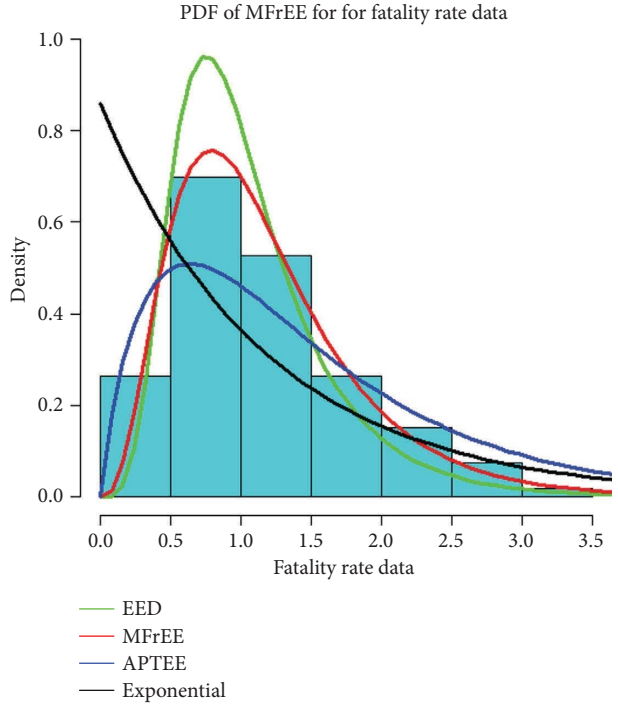

Figure 12: Plots for the fitted MFrEE pdf and other models to the fatality rate patient data.

Table 7: Estimates of fitted distributions for fatality rate data.

Model	$\hat{\alpha}$	$\hat{\lambda}$	$\hat{\gamma}$
EED (base)	4.028373	1.797765	
MFrEE	1.759827	3.814093	3.328963
APTEE	0.9984518	0.9474172	2.2988713
Exponential		0.8587129	

Table 8: Model comparison criteria for fatality rate data.

Model	AIC	CAIC	BIC	HQIC	KS value	p-value
EED (basic)	195.64	195.87	203.63	198.88	91.13	0.0510
MFrEE	186.25	186.36	191.57	188.41	91.13	0.7710
APTEE	216.77	217.00	224.76	220	105.39	0.0023
Exponential	246.29	246.33	248.96	247.38	122.15	0.000

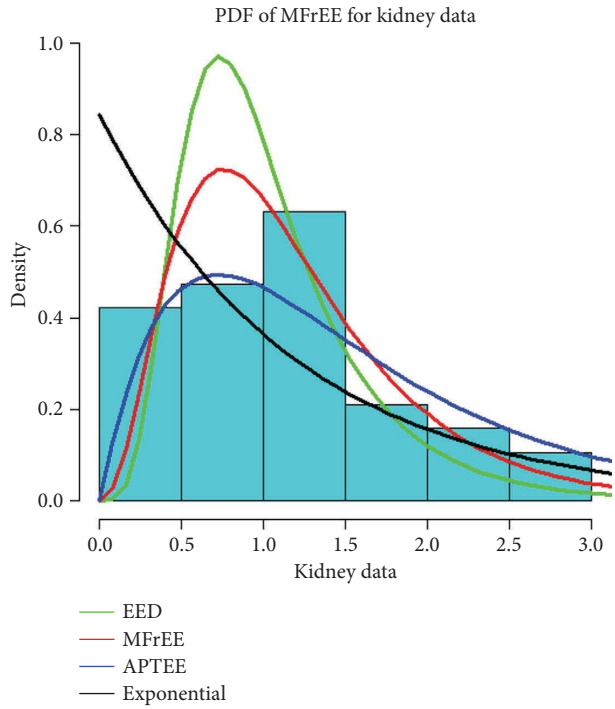

Figure 13: Plots for the fitted MFrEE pdf and other models to the kidney data.

BIC = 191.57, HQIC = 188.41). These lower scores indicate that, compared with the baseline EED, APTEE, and exponential models, the MFrEE model provides a more accurate and parsimonious representation of the underlying data.

Regarding goodness-of-fit, the KS statistic and its corresponding p-value also support the superior performance of MFrEE. Although the KS statistic for MFrEE (91.13) is equal to that of the baseline EED model, the p-value for MFrEE is substantially higher (0.7710). This value is far above the conventional significance threshold ($\alpha = 0.05$), indicating no evidence against the null hypothesis that the data follow the MFrEE distribution. In contrast, the p-values for APTEE (0.0023) and Exponential (0.000) are extremely small, showing a clear lack of fit.

The high p-value (0.7710) suggests excellent agreement between the empirical and fitted MFrEE distribution, confirming its suitability for the fatality rate data. It reflects a very small distance between the empirical and theoretical distributions in the KS test.

Overall, both the information criteria and KS goodness-of-fit results clearly demonstrate that the MFrEE model provides the best fit for the fatality rate dataset, outperforming all competing models in terms of accuracy, efficiency, and goodness-of-fit.

The proposed MFrEE distribution is fully defined and thoroughly described in this study. Both simulation studies and real-data applications demonstrate the model's flexibility and promising performance. Based on these results, we

recommend applying the MFrEE distribution to real-world datasets in fields such as health, engineering, and economics to further validate its practical utility.

4. Conclusions

This paper introduces a novel probability model, the MFrEE distribution, and provides a comprehensive study of its properties. We derive the PDF, CDF, survival function, and hazard function and illustrate these functions across different parameter values. Key distributional characteristics, including moments, mean, variance, mode, quantiles, skewness, kurtosis, and the MGF, were also derived and examined. Random samples from the MFrEE distribution were generated using the AR method, and parameters were estimated via MLE. The performance of the estimators was further assessed through Monte Carlo simulations based on bias, MSE, and CP, with CP values remaining close to the nominal 95% level across scenarios.

The model's empirical applicability was demonstrated using three real-world datasets, where it achieved superior fit compared to existing models, as indicated by consistently lower values of AIC, BIC, and AICc. Notably, the MFrEE distribution exhibits a flexible hazard function capable of modeling monotonic, bathtub, and unimodal shapes, making it highly suitable for applications in health, engineering, science, and economics, particularly for lifetime and reliability data.

In conclusion, the MFrEE distribution represents a significant contribution to probability theory and statistical modeling. Future research may focus on applying the model to additional real-world datasets and exploring machine learning–based approaches for parameter estimation, comparing their performance against the MLE approach used in this study.

Moreover, future research could examine application areas where flexible hazard rate structures provide substantial practical benefit. Potential domains include biomedical and clinical survival analysis, engineering reliability assessments, environmental risk and extreme-event modeling, actuarial science, and financial duration analysis. Investigating these areas would deepen understanding of the model's versatility and highlight its advantages over competing lifetime distributions in complex real-data settings.

Data Availability Statement

Data sharing is not applicable to this article as no new data were created or analyzed in this study.

Ethics Statement

The authors have nothing to report.

Disclosure

All authors read and approved the final version of the manuscript.

Conflicts of Interest

The authors declare no conflicts of interest.

Author Contributions

All authors meet the Wiley criteria for authorship. Merga Abdissa Aga conceptualized the study, performed the data analysis, and drafted the manuscript. Shibiru Jabessa Dugasa contributed to the study design and assisted with data interpretation. Habte Tadese and Ding-Geng Chen provided guidance on the methodology, critically reviewed the manuscript, and contributed to the interpretation of the results.

Funding

This research did not receive any specific grant from funding agencies in the public, commercial, or not-for-profit sectors.

References

[1] J. F. Lawless, *Statistical Models and Methods for Lifetime Data*, 2nd ed. (Wiley, 2003).

[2] R. D. Gupta and D. Kundu, "Generalized Exponential Distributions," *Australian & New Zealand Journal of Statistics* 41, no. 2 (1999): 173–188, https://doi.org/10.1111/1467-842x.00072.

[3] G. S. Mudholkar, D. K. Srivastava, and M. Freimer, "The Exponentiated Weibull Family: A Reanalysis of the Bus-Motor-Failure Data," *Technometrics* 37, no. 4 (1995): 436–445, https://doi.org/10.1080/00401706.1995.10484376.

[4] S. Nadarajah and S. Kotz, "The Exponentiated Type Distributions," *Acta Applicandae Mathematica* 92, no. 2 (2006): 97–111, https://doi.org/10.1007/s10440-006-9055-0.

[5] G. S. Mudholkar and D. K. Srivastava, "Exponentiated Weibull Family for Analyzing Bathtub Failure-Rate Data," *IEEE Transactions on Reliability* 42, no. 2 (1993): 299–302, https://doi.org/10.1109/24.229504.

[6] C. D. Lai and M. Xie, *Stochastic Ageing and Dependence for Reliability* (Springer, 2006).

[7] A. W. Marshall and I. Olkin, "A New Method for Adding a Parameter to a Family of Distributions With Applications to the Exponential and Weibull Families," *Biometrika* 84, no. 3 (1997): 641–652.

[8] A. Alzaatreh, C. Lee, and F. Famoye, "A New Method for Generating Families of Continuous Distributions," *Metron* 71, no. 1 (2013): 63–79, https://doi.org/10.1007/s40300-013-0007-y.

[9] M. C. Jones, "Families of Distributions Arising From Distributions of Order Statistics," *Test* 13, no. 1 (2004): 1–43, https://doi.org/10.1007/bf02602999.

[10] G. M. Cordeiro and M. de Castro, "A New Family of Generalized Distributions," *Journal of Statistical Computation and Simulation* 81, no. 7 (2011): 883–898, https://doi.org/10.1080/00949650903530745.

[11] K. Keganne, L. Gabaitiri, and B. Makubate, "A New Extension of the Exponentiated Generalized-G Family of Distributions," *Scientific African* 20 (2023): e01719, https://doi.org/10.1016/j.sciaf.2023.e01719.

[12] A. Alzaghal, F. Famoye, and C. Lee, "Exponentiated TX Family of Distributions With Some Applications,"

International Journal of Statistics and Probability 2, no. 3 (2013): 31.

[13] C. Lee, F. Famoye, and A. Y. Alzaatreh, "Methods for Generating Families of Univariate Continuous Distributions in the Recent Decades," *Wiley Interdisciplinary Reviews: Computational Statistics* 5, no. 3 (2013): 219–238, https://doi.org/10.1002/wics.1255.

[14] Z. Ahmad, M. Elgarhy, and N. Abbas, "A New Extended Alpha Power Transformed Family of Distributions: Properties and Applications," *Journal of Statistical Modelling: Theory and Applications* 1, no. 2 (2018): 1–16.

[15] Z. Ahmad, M. Elgarhy, G. G. Hamedani, and N. Sh. Butt, "Odd Generalized N-H Generated Family of Distributions With Application to Exponential Model," *Pakistan Journal of Statistics and Operation Research* 16, no. 1 (2020): 53–71, https://doi.org/10.18187/pjsor.v16i1.2295.

[16] A. S. Al-Moisheer, I. Elbatal, W. Almutiry, and M. Elgarhy, "Odd Inverse Power Generalized Weibull Generated Family of Distributions: Properties and Applications," *Mathematical Problems in Engineering* 2021 (2021): 5082192–17, https://doi.org/10.1155/2021/5082192.

[17] A. M. Almarashi and M. Elgarhy, "A New Muth Generated Family of Distributions With Applications," *Journal of Nonlinear Science and Applications* 11, no. 10 (2018): 1–18, https://doi.org/10.22436/jnsa.011.10.06.

[18] A. M. Almarashi, F. Jamal, C. Chesneau, and M. Elgarhy, "A New Truncated Muth Generated Family of Distributions With Applications," *Complexity* 2021, no. 1 (2021): 1211526, https://doi.org/10.1155/2021/1211526.

[19] S. A. Alyami, M. G. Babu, I. Elbatal, N. Alotaibi, and M. Elgarhy, "Type II Half-Logistic Odd Fréchet Class of Distributions: Statistical Theory and Applications," *Symmetry* 14, no. 6 (2022): 1222, https://doi.org/10.3390/sym14061222.

[20] S. A. Alyami, I. Elbatal, N. Alotaibi, E. M. Almetwally, and M. Elgarhy, "Modeling to Factor Productivity of the United Kingdom Food Chain: Using a New Lifetime-Generated Family of Distributions," *Sustainability* 14 (2022): 8942, https://doi.org/10.3390/su14148942.

[21] S. Benchiha, L. P. Sapkota, A. Al Mutairi, et al., "A New Sine Family of Generalized Distributions: Statistical Inference With Applications," *Mathematical and Computational Applications* 28, no. 4 (2023): 83, https://doi.org/10.3390/mca28040083.

[22] I. Elbatal, M. Elgarhy, and B. M. G. Kibria, "Alpha Power Transformed Weibull-g Family of Distributions: Theory and Applications," *Journal of Statistical Theory and Applications* 20, no. 2 (2021): 340–354, https://doi.org/10.2991/jsta.d.210222.002.

[23] C. Chesneau, C. Tanış, H. S. Bakouch, and N. Qarmalah, "A General Weighted Exponentiated Family of Distributions With Application to Carbon Fiber and Petroleum Rock Data," *Lobachevskii Journal of Mathematics* 44, no. 11 (2023): 4663–4675, https://doi.org/10.1134/s1995080223110100.

[24] A. S. Hassan, N. Alsadat, M. Elgarhy, C. Chesneau, and H. F. Nagy, "Analysis of R=P[Y<X<Z] Using Ranked Set Sampling for a Generalized Inverse Exponential Model," *Axioms* 12, no. 3 (2023): 302, https://doi.org/10.3390/axioms12030302.

[25] B. Saraçoğlu and C. Tanış, "A New Lifetime Distribution: Transmuted Exponential Power Distribution," *Communications Faculty of Sciences University of Ankara Series A1 Mathematics and Statistics* 70, no. 1 (2021): 1–14, https://doi.org/10.31801/cfsuasmas.528306.

[26] A. A. H. Ahmadini, M. H. Tahir, O. Alamri, A. Munawar, and M. Elgarhy, "Robust Assessment on the Developments of Three Extended Exponential Models With Some New Properties and Applications," *Mathematical Problems in Engineering* 2021 (2021): 1871962–16, https://doi.org/10.1155/2021/1871962.

[27] A. A. Al-Babtain, I. Elbatal, C. Chesneau, and M. Elgarhy, "On a New Modeling Strategy: The logarithmically-Exponential Class of Distributions," *AIMS Mathematics* 6, no. 7 (2021): 7845–7871, https://doi.org/10.3934/math.2021456.

[28] M. H. Alabdulhadi, A. R. El-Saeed, M. Elgarhy, A. E. H. Eisa, and D. A. Abdo, "Statistical Inference of Marshall-Olkin Extended Exponential Distribution Based on Progressively Type-I Censored Data," *Applied Mathematics & Information Sciences* 17, no. 6 (2023): 1033–1046.

[29] A. S. Alghamdi, "Marshall–Olkin Exponentiated Inverse Rayleigh Distribution Using Bayesian and Non-Bayesian Estimation Methods," *Symmetry* 17, no. 5 (2025): 707, https://doi.org/10.3390/sym17050707.

[30] R. Alotaibi, M. Nassar, H. Rezk, and A. Elshahhat, "Inferences and Engineering Applications of Alpha Power Weibull Distribution Using Progressive Type-II Censoring," *Mathematics* 10, no. 16 (2022): 2901, https://doi.org/10.3390/math10162901.

[31] E. A. Eldessouky, O. H. M. Hassan, M. Elgarhy, E. A. A. Hassan, I. Elbatal, and E. M. Almetwally, "A New Extension of the Kumaraswamy Exponential Model with Modeling of Food Chain Data," *Axioms* 12, no. 4 (2023): 379, https://doi.org/10.3390/axioms12040379.

[32] A. M. Gemeay, S. O. Bashiru, L. P. Sapkota, M. Kayid, S. Dutta, and S. Mohammad, "A New Power Transformed Distribution With Applications to Radiotherapy and Environmental Datasets," *Journal of Radiation Research and Applied Sciences* 18, no. 2 (2025): 101339, https://doi.org/10.1016/j.jrras.2025.101339.

[33] A. S. Hassan, R. E. Mohamd, M. Elgarhy, and A. Fayomi, "Alpha Power Transformed Extended Exponential Distribution: Properties and Applications," *The Journal of Nonlinear Science and Applications* 12, no. 4 (2018): 62–67, https://doi.org/10.22436/jnsa.012.04.05.

[34] F. Jamal, S. Kanwal, S. Shafiq, et al., "The New Extended Exponentiated Burr XII Distribution: Properties and Applications," *Journal of Radiation Research and Applied Sciences* 18, no. 1 (2025): 101200, https://doi.org/10.1016/j.jrras.2024.101200.

[35] I. E. Ragab, N. Alsadat, O. S. Balogun, and M. Elgarhy, "Unit Extended Exponential Distribution With Applications," *Journal of Radiation Research and Applied Sciences* 17, no. 4 (2024): 101118, https://doi.org/10.1016/j.jrras.2024.101118.

[36] M. Shrahili, I. Elbatal, W. Almutiry, and M. Elgarhy, "Estimation of Sine Inverse Exponential Model Under Censored Schemes," *Journal of Mathematics* 2021 (2021): 7330385–7330389, https://doi.org/10.1155/2021/7330385.

[37] I. V. Omekam, O. I. Adeniyi, and A. O. Adejumo, "Modified Frechet Distributions and Their Generalized Families," *Science World Journal* 17, no. 2 (2022): 338–245.

[38] A. Khalil, A. A. H. Ahmadini, M. Ali, W. K. Mashwani, S. S. Alshqaq, and Z. Salleh, "A Novel Method for Developing Efficient Probability Distributions With Applications to

Engineering and Life Science Data," *Journal of Mathematics* 2021 (2021): 1–13, https://doi.org/10.1155/2021/4479270.

[39] H. S. Klakattawi, A. A. Khormi, and L. A. Baharith, "The New Generalized Exponentiated Fréchet–Weibull Distribution: Properties, Applications, and Regression Model," *Complexity* 2023, no. 1 (2023): 2196572.

[40] J. K. Pillai and G. B. Moolath, "A New Generalization of the Fréchet Distribution: Properties and Application," *Statistica* 79, no. 3 (2019): 267–289.

[41] E. A. Hussein, H. M. Aljohani, and A. Z. Afify, "The Extended Weibull-Frechét Distribution: Properties, Inference, and Applications in Medicine and Engineering," *AIMS Mathematics* 7, no. 1 (2021): 225–246, https://doi.org/10.3934/math.2022014.

[42] H. Cramér, *Mathematical Methods of Statistics* (Princeton University Press, 1999).

[43] C. R. Rao, C. R. Rao, M. Statistiker, C. R. Rao, and C. R. Rao, *Linear Statistical Inference and Its Applications* (Wiley, 1973).

[44] E. L. Lehmann and G. Casella, *Theory of Point Estimation* (Springer, 1998).

[45] C. McGilchrist and C. Aisbett, "Regression With Frailty in Survival Analysis," *Biometrics* 47, no. 2 (1991): 461–466, https://doi.org/10.2307/2532138.

[46] D. N. P. Murthy, M. Xie, and R. Jiang, *Weibull Models* (Wiley, 2004).

[47] H. F. Cordero-Franco, F. J. Guzmán-de la Garza, and A. M. Salinas-Martínez, "COVID-19 Fatality Rate Conditioned by Risk Factors in Mexico in 2020," *Revista medica del Instituto Mexicano del Seguro Social* 62, no. 5 (2024): 1–7.